UCID-17359

Lawrence Livermore Laboratory

TEMPERATURE JUMP BOUNDARY CONDITIONS IN RADIATION DIFFUSION

C. T. Alonso

December, 1976

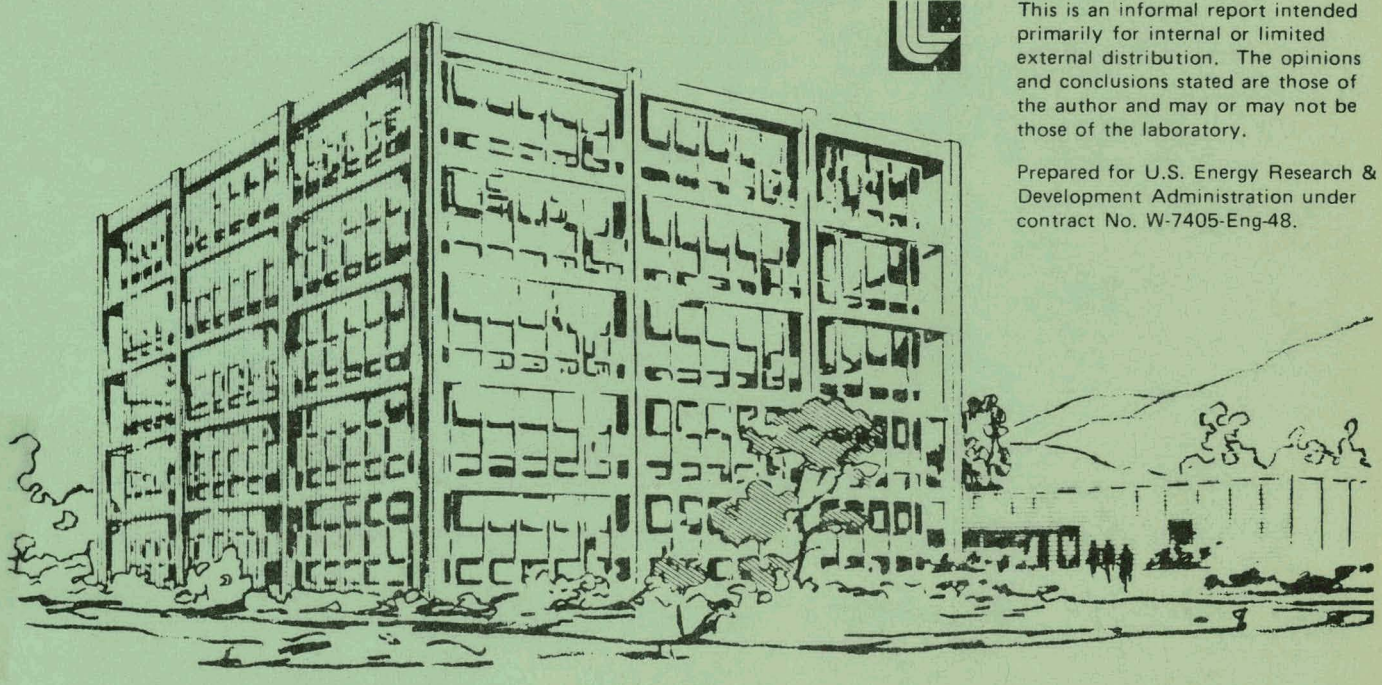

Prepared for U.S. Energy Research & Development Administration under contract No. W-7405-Eng-48.

DISCLAIMER

TEMPERATURE JUMP BOUNDARY CONDITIONS IN RADIATION DIFFUSION

C. T. Alonso

University of California, Lawrence Livermore Laboratory

Livermore, California 94550

December, 1976

ABSTRACT

The radiation diffusion approximation greatly simplifies radiation transport problems. Yet the application of this method has often been unnecessarily restricted to optically thick regions, or has been extended through the use of such ad hoc devices as flux limiters [13, 14]. The purpose of this paper is to review and draw attention to the use of the more physically appropriate temperature jump boundary conditions for extending the range of validity of the diffusion approximation. Pioneering work by Deissler [3], Siegel and Howell [7], and others [9, 10, 11] has shown that temperature jump boundary conditions remove the singularity in flux that occurs in ordinary diffusion at small optical thicknesses. In this review paper Deissler's equations for frequency-dependent jump boundary conditions are presented and specific geometric examples are calculated analytically for steady state radiation transfer. When jump boundary conditions are applied to radiation diffusion, they yield exact solutions which are naturally flux- limited and geometry-corrected. We believe that the presence of temperature jumps on source boundaries is probably responsible in some cases for the past need for imposing ad hoc flux-limiting constraints [13, 14] on pure diffusion solutions. The solution for transfer between plane slabs, which is exact to all orders of optical thickness, also provides a useful tool for studying the accuracy of computer codes.

TABLE OF CONTENTS

I. INTRODUCTION: TEMPERATURE JUMP IN THE BOUNDARY LAYER OF RAREFIED GASES

Temperature jump [1] is a well-established phenomenon in the molecular dynamics of rarefied gases (gases whose Knudsen number $Kn = \lambda/L$ is not small, where λ is the molecular mean free path and L is a characteristic dimension of the container). In one of the most celebrated examples of this phenomenon, Millikan found it necessary to correct for the associated "velocity slip" in his oil drop experiments [2]. In this introductory section, temperature jump and velocity slip will be described qualitatively for the case of rarefied gases, and then in the next section the quantitative equations for radiation transfer with temperature jump, as derived by Deissler [3], will be presented and explored.

Consider a gas at temperature T_g flowing past a wall at temperature T_w as in Fig. 1. On the average, a gas molecule hits the wall as a result of a collision that occurred a distance λ from the wall. First consider the case of isentropic gas flow with specular reflection. Since the interaction with the wall is elastic, the magnitudes of the velocity components of a molecule are not changed during the specular reflection, and therefore the reflected molecules display the same Maxwellian distribution as the incident molecules. That is, specular reflection does not permit any adjustment of the mass velocity and temperature of the gas toward that of the wall. It implies perfect slip flow and no accommodation between the temperatures of the gas and the boundary.

Now consider nonisentropic flow and diffuse reflection. In this case the molecules strike the boundary with complete loss of the tangential

components of velocity, and they escape from the wall after attaining either partial or complete thermal equilibrium with the wall. The direction of emission is independent of the incident direction. Since the reflected molecules come off the wall in a Maxwellian (or perhaps even non-Maxwellian) distribution which corresponds to a temperature that is different from both the gas temperature T_g and the wall temperature T_w, there is formed adjacent to the wall a boundary layer with a non-Maxwellian molecular distribution. The requirement that flux be continuous over the boundary results in a discontinuity in temperature and velocity over the boundary layer. This "temperature jump" is shown schematically in Fig. 1.

In one of the first considerations of temperature jump, Maxwell [4] introduced a coefficient f which is the fraction of incident molecules that are diffusely reflected, and therefore (1 - f) is the fraction that are specularly reflected. Subsequent experiments by Millikan [2] verified the existence of f in rarefied gas flow. Present-day experiments measure this "coefficient of slip flow" very accurately for various materials.

Velocity slip occurs over a distance of the order of the mean free path. If the Knudsen number is small, the temperature and velocity discontinuities are negligibly small and ordinary continuum descriptions such as pure diffusion are accurate. But when the Knudsen number is around unity, the effect of temperature jump becomes very important. In gases at extremely high Knudsen numbers, the reflected stream of molecules does not interact much with the incident stream. This represents yet another flow regime generally referred to as "free molecular flow". In Fig. 2 these flow regions are illustrated schematically for a typical gas.

Perhaps the simplest quantitative example of slip flow is exhibited by a gas streaming slowly through a tube. If the molecules are diffusely reflected from the walls, kinetic theory shows that the flux of molecules hitting the wall from a gas at rest is $\phi = 1/4\ nc$ where n is the particle density and c is the mean velocity. If the molecules have an average mass motion $v << c$ parallel to the wall, the tangential momentum imparted to the wall is $1/4\ ncmv$. But since the boundary layer is made up half of incident molecules entering with the tangential velocity v and half of diffusely reflected molecules with zero average tangential velocity, the average tangential velocity of the layer is $v_0 = v/2$ and the tangential momentum imparted to the wall is really $P = 1/2\ nmcv_0$. If the viscosity away from the wall is η and the effective friction of the boundary layer is β, the coefficient of slip is defined by $\zeta = \eta/\beta$. But the coefficient of friction β is just the tangential pressure P divided by v_0, i.e., $\beta = 1/2\ nmc$. Since from kinetic theory $\eta \sim nmc\lambda$ we therefore find that $\zeta \sim \lambda$. That is, the coefficient of slip is proportional to the mean free path.

The above examples illustrate the physical meaning of temperature jump and velocity slip in molecular flow. An analogous situation occurs when the molecules are replaced by photons streaming through a transparent medium. In a manner entirely similar to the molecular case, conservation of flux at a source boundary can result in a temperature discontinuity at that boundary. In the simplest example, if the walls of the medium are black, the directionality of the incident flux is lost and the photons are diffusely reemitted. In the next simplest example, if the walls are grey (i.e., their emissivity and absorptivity do not depend on angle or frequency, but do

depend on temperature), then since the grey surface is not a perfect absorber only part of its incident photon flux is diffusely reflected. When the "photon Knudsen number" λ_γ/L is of the order of unity, the non-Planckian distribution of diffusely reflected photons creates a boundary layer with temperature jump at a source boundary. The flux across the boundary is continuous but the temperature is not. In the next section the radiative transfer equations for such a "Knudsen radiation field" are examined.

II. TEMPERATURE JUMP IN THE RADIATION DIFFUSION APPROXIMATION

In this section exact solutions to the diffusion equation will be explored in the light of jump boundary conditions. Although the emphasis will be on steady state solutions, many of the radiative heat balances considered here are not limited to steady state conditions.

The second-order steady state diffusion equation was first derived by Rosseland [5] and can be written

$$q_z = \frac{-4}{3\kappa_\nu} \frac{\partial e_\nu}{\partial z} \tag{1}$$

where q_z is the flux in the z-direction, κ_ν is the absorption coefficient at frequency ν (opacity = $1/\kappa\rho$), and e_ν is the spectral emissive power given by Planck's distribution function.

Referring to the geometry shown in Fig. 3, consider radiation originating at volume element dV and streaming through area dA at point $(x_0\ y_0\ z_0)$. Suppose dA is close to a wall in the x-y plane. Then the

jump boundary conditions that apply to Eq. (2) at the wall were derived by Deissler [3] (see Appendix A) and they can be written in the following frequency-dependent form for the temperature jump to second order:

$$\pm (e_{\omega} - e_{\nu 0}) = \left(\frac{1}{\varepsilon} - \frac{1}{2}\right) q_{z0} \pm \frac{1}{4\kappa_{\nu}^2} \left(2 \left.\frac{\partial^2 e_{\nu}}{\partial z^2}\right|_0 + \left.\frac{\partial^2 e_{\nu}}{\partial y^2}\right|_0 + \left.\frac{\partial^2 e_{\nu}}{\partial x^2}\right|_0 \right) \qquad (2)$$

where e_{ω} is the emissive power (σT^4) of the wall, e_{ν} is the emissive power at frequency ν of the transparent medium adjacent to the wall, and ε is the wall emissivity (i.e., the ratio of the actual emitted energy of the wall to its emitted energy if the wall were a blackbody). (Emissivities are normally deduced from the measured spectra of radiating objects, and emissivities often approach unity as high temperatures are attained.) The + sign applies to a wall <u>below</u> dA and the minus sign to a wall <u>above</u> dA. The subscript "0" implies evaluation in the transparent medium infinitesimally close to the wall. Even when there is no opaque wall, similar equations for discontinuities in emissive power between two absorbing-emitting media with sources or sinks can be derived in the same manner. On the other hand, boundaries between stagnant absorbing-emitting regions with no sources or sinks do not generate a temperature jump [6].

If Eqs. (1) and (2) are required in a frequency-independent form, they can be integrated over all frequencies to obtain the total radiative flux and the total emissive power. Writing Planck's distribution function in the form

$$e_\nu = \frac{2\pi h\nu^3}{c^2 \exp\left[h\nu\sigma^{1/4} k^{-1} e^{-1/4}\right] - 1} , \tag{3}$$

where e with no subscript ν represents the total emissive power (σT^4) of the transparent medium, Eq. (1) can be integrated to yield

$$q_z = \frac{-4}{3\kappa_r} \frac{\partial e}{\partial z} \tag{4}$$

where $e = \sigma T^4$ and κ_r is the Rosseland mean absorption coefficient

$$\frac{1}{\kappa_r} = \int_0^\infty \frac{1}{\kappa_\nu} \frac{\partial e_\nu}{\partial e} d\nu . \tag{5}$$

Similarly Eq. (2) can be integrated with the help of (3) to give

$$\pm (e_\omega - e) = \left(\frac{1}{\epsilon} - \frac{1}{2}\right) q_{z0} \pm \frac{1}{4\kappa_s^2} \left(2 \left.\frac{\partial^2 e}{\partial z^2}\right|_0 + \left.\frac{\partial^2 e}{\partial y^2}\right|_0 + \left.\frac{\partial^2 e}{\partial x^2}\right|_0 \right)$$
$$\pm \frac{I}{4} \left[2\left(\frac{\partial e}{\partial z}\right)_0^2 + \left(\frac{\partial e}{\partial y}\right)_0^2 + \left(\frac{\partial e}{\partial x}\right)_0^2 \right] \tag{6}$$

where

$$\frac{1}{\kappa_s^2} = \int_0^\infty \frac{1}{\kappa_\nu^2} \frac{\partial e_\nu}{\partial e} d\nu \tag{7}$$

and

$$I = \int_0^\infty \frac{1}{\kappa_\nu^2} \frac{\partial^2 e_\nu}{\partial e^2} d\nu . \tag{8}$$

For a grey medium, κ_ν is independent of ν and $I = 0$. Equations (1)-(2) can be used directly in frequency-dependent diffusion codes; Eqs. (4)-(8) can be used in single group diffusion codes.

The jump boundary conditions (2) and (6) play the same role as flux limiters, but instead of being ad hoc corrections they are exact to second order (see Appendix A). It is our belief that the jump boundary conditions represent at least partly the physical origin of the necessity for imposing flux limiting constraints on pure diffusion solutions.

In the next section we shall present three specific examples of the use of these equations for the problems of transfer between (1) plane slabs, (2) concentric cylinders, and (3) concentric spheres.

III. TRANSFER BETWEEN PLANE SLABS, CONCENTRIC SPHERES, AND CONCENTRIC CYLINDERS SEPARATED BY AN ABSORBING MEDIUM

The use of Eqs. (4)-(8) is straightforward. Consider first the infinite parallel plane slabs shown in Fig. 4(a). The gap between the slabs, of width L, is filled with an absorbing medium with Rosseland absorption coefficient κ_r. In this case the steady state flux q is independent of z and Eq. (4) is integrated to give

$$e_1 - e = \frac{3\kappa_r}{4} qz \tag{9}$$

or

$$\frac{e_1 - e_2}{q} = \frac{3\kappa L}{4} \tag{10}$$

where e_1 and e_2 are the emissive powers of the transparent medium arbitrarily

close to walls 1 and 2 respectively. The energy jumps at the walls become, from Eqs. (6)-(8),

$$\frac{e_{\omega 1} - e_1}{q} = \frac{1}{\varepsilon_1} - \frac{1}{2} + \frac{9}{32} \kappa_r^2 \, q \, I \tag{11}$$

at wall 1 and

$$\frac{e_2 - e_{\omega 2}}{q} = \frac{1}{\varepsilon_2} - \frac{1}{2} - \frac{9}{32} \kappa_r^2 \, q \, I \tag{12}$$

at wall 2.

Assuming a grey medium ($I = 0$) and adding Eqs. (10)-(12) gives

$$\frac{q}{\sigma(T_1^4 - T_2^4)} = \frac{1}{\frac{3\kappa L}{4} + \frac{1}{\varepsilon_1} + \frac{1}{\varepsilon_2} - 1} \tag{13}$$

where T_1 and T_2 are the wall temperatures. This ratio represents an exact expression for the flux between parallel slabs through a material of opacity $1/\kappa\rho$. In this case all derivatives of order greater than second vanish, so Eq. (13) is exact to all orders and for all optical thicknesses. If the walls are perfect blackbodies ($\varepsilon_1 = \varepsilon_2 = 1$) then this expression reduces to the Milne boundary condition

$$\frac{q}{\sigma(T_1^4 - T_2^4)} = \frac{1}{1 + \frac{3\kappa L}{4}} \tag{14}$$

Equation (13) also reduces to the correct form in the case of infinitely small optical thickness κL. The exact solution for the flux as a function

of optical thickness κL is shown in Fig. 5. Also shown is the pure diffusion solution without boundary conditions, viz. Eq. (10). At large values of κL the pure diffusion solution becomes exact. The effectiveness of the jump boundary condition as a flux limiter is obvious.

The corresponding temperature distribution in an absorbing material between two slabs is given by

$$\frac{T^4(z) - T_2^4}{T_1^4 - T_2^4} = \frac{\frac{3\kappa L}{4}\left(1 - \frac{z}{L}\right) + \frac{1}{\epsilon_2} - \frac{1}{2}}{\frac{3\kappa L}{4} + \frac{1}{\epsilon_1} + \frac{1}{\epsilon_2} - 1} \quad .$$

This distribution is shown as a function of z and of the optical thickness κL in Fig. 9. The definition of temperature in a vacuum ($\kappa L = 0$) is obscure, but these equations yield the average wall temperature throughout in that limit. The actual temperature jump at the walls is given in Fig. 10 as a function of optical thickness.

In the case of radiating concentric spheres such as in Fig. (4b), the flux q is proportional to $1/r^2$ and so integration of (4) gives

$$e - e_1 = \frac{3\kappa_r}{4} q_1 r_1^2 \left(\frac{1}{r} - \frac{1}{r_1}\right) \tag{15}$$

where q_1 is the steady state flux emitted by surface 1. Using $r^2 = x^2 + y^2 + z^2$, the derivatives in the jump boundary conditions (6) may be evaluated at walls 1 and 2 to give

$$\frac{e_{\omega 1} - e_1}{q_1} = \left(\frac{1}{\epsilon_1} - \frac{1}{2}\right) + \frac{3}{8}\frac{\kappa_r}{\kappa_B^2 r_1} + \frac{9}{32} I\, q_1\, \kappa_r^2 \tag{16}$$

and

$$\frac{e_2 - e_{\omega 2}}{q_1} = \left(\frac{1}{\epsilon_2} - \frac{1}{2}\right)\left(\frac{r_1}{r_2}\right)^2 - \frac{3}{8}\frac{\kappa r_1^2}{\kappa_s^2 r_2^3} - \frac{9}{32} q_1 \kappa_r^2 I \left(\frac{r_1}{r_2}\right)^4 \tag{17}$$

Adding Eqs. (15)-(17), the final expression for the inverse of the steady state flux between concentric radiating spheres is

$$\frac{\sigma(T_1^4 - T_2^4)}{q_1} = \frac{3\kappa_r r_1}{4}\left(1 - \frac{r_1}{r_2}\right) + \left(\frac{1}{\epsilon_1} - \frac{1}{2}\right) + \left(\frac{1}{\epsilon_2} - \frac{1}{2}\right)\left(\frac{r_1}{r_2}\right)^2$$
$$+ \frac{3}{8}\left(\frac{\kappa_r}{\kappa_s}\right)^2 \frac{1}{\kappa_r r_1}\left[1 - \left(\frac{r_1}{r_2}\right)^3\right] + \frac{9}{32} I q_1 \kappa_r^2 \left[1 - \left(\frac{r_1}{r_2}\right)^4\right] \tag{18}$$

Note that this is parameterized in terms of the ratio of the radii (r_1/r_2) and the quantity κ_{r_1}. In terms of the optical thickness $\kappa L = \kappa(r_2 - r_1)$ Eq. (18) becomes (where κ is meant to be the Rosseland absorption coefficient κ_r)

$$\frac{\sigma(T_1^4 - T_2^4)}{q_1} = \frac{3\kappa L}{4}\left(\frac{r_1}{r_2}\right) + \left(\frac{1}{\epsilon_1} - \frac{1}{2}\right) + \left(\frac{1}{\epsilon_2} - \frac{1}{2}\right)\left(\frac{r_1}{r_2}\right)^2$$
$$+ \frac{3}{8}\left(\frac{\kappa}{\kappa_s}\right)^2 \frac{1}{\kappa L}\left(\frac{r_2}{r_1} - 1\right)\left[1 - \left(\frac{r_1}{r_2}\right)^3\right]$$
$$+ \frac{9}{32} I q_1 (\kappa L)^2 r_1^2 \left(\frac{r_2}{r_1} - 1\right)^2 \left[1 - \left(\frac{r_1}{r_2}\right)^4\right]. \tag{19}$$

The correct solution for the flux between empty concentric spheres is [7]

$$\frac{\sigma(T_1^4 - T_2^4)}{q_1} = \frac{1}{\epsilon_1} + \left(\frac{r_1}{r_2}\right)^2 \left(\frac{1}{\epsilon_2} - 1\right) \quad . \tag{20}$$

For comparison, in the limit of small optical thickness and a grey medium (I = 0), Eq. (19) reduces to

$$\lim_{\kappa L \to 0} \frac{\sigma(T_1^4 - T_2^4)}{q_1} = \left(\frac{1}{\varepsilon_1} - \frac{1}{2}\right) + \left(\frac{1}{\varepsilon_2} - \frac{1}{2}\right)\left(\frac{r_1}{r_2}\right)^2 + \frac{3}{8}\left(\frac{\kappa}{\kappa_s}\right)^2 \lim_{\kappa L \to 0} \frac{1}{\kappa L}\left(\frac{r_2}{r_1} - 1\right)\left[1 - \left(\frac{r_1}{r_2}\right)^3\right] \tag{21}$$

This should be identical to Eq. (20). Therefore the second-order solution (19) is exactly correct only for $r_1 \to r_2$, and its accuracy goes as $(r_1/r_2)^2$. The second-order sphere solution is not exact, as it was in the case of slab flow, because the higher order derivatives do not vanish in the case of concentric spheres.

The steady state temperature distribution can be calculated from (15)-(17) with the use of (18) for q_1:

$$\frac{\sigma(T^4(r) - T_2^4)}{q_1} = \frac{3\kappa}{4} r_1^2 \left(\frac{1}{r} - \frac{1}{r_2}\right) + \left(\frac{1}{\varepsilon_2} - \frac{1}{2}\right)\left(\frac{r_1}{r_2}\right)^2 - \frac{3}{8}\frac{\kappa_r}{\kappa_s^2}\frac{r_1^2}{r_2^3} - \frac{9}{32} q_1 \kappa_r^2 I \left(\frac{r_1}{r_2}\right)^4 \tag{22}$$

In the limit of blackbody walls ($\varepsilon_1 = \varepsilon_2 = 1$) and a grey medium (I = 0) the solution for concentric spheres becomes, assuming $\kappa_r \cong \kappa_s$,

$$\frac{\sigma(T_1^4 - T_2^4)}{q_1} = \frac{3\kappa L}{4}\frac{r_1}{r_2} + \frac{1}{2}\left[1 + \left(\frac{r_1}{r_2}\right)^2\right] + \frac{3}{8}\frac{1}{\kappa L}\left(\frac{r_2}{r_1} - 1\right)\left[1 - \left(\frac{r_1}{r_2}\right)^3\right] \tag{23}$$

for the flux ($q(r) = q_1 r_1^2/r^2$) and

$$\frac{\sigma(T^4 - T_2^4)}{q_1} = \frac{3\kappa}{4} r_1^2 \left(\frac{1}{r} - \frac{1}{r_2}\right) + \frac{1}{2}\left(\frac{r_1}{r_2}\right)^2 - \frac{3}{8}\frac{1}{\kappa r_1}\left(\frac{r_1}{r_2}\right)^3 \tag{24}$$

for the temperature distribution. These temperature distributions, which are hyperbolae in T^4 and r, are shown in Fig. 11 for the case $r_1/r_2 = 0.75$.

The flux from Eq. (23) is plotted as a function of optical thickness κL in Fig. 6 for several values of r_1/r_2. Again the jump boundary conditions provide a very effective flux limiter. When $r_1 = r_2$ the Milne condition is retrieved.

Finally, the corresponding equations for concentric cylinders, as shown in Fig. 4(c), are

$$\frac{e - e_1}{q_1} = \frac{3\kappa r_1}{4} \ln \frac{r_2}{r_1} \tag{25}$$

with boundary conditions

$$\frac{e_{\omega 1} - e_1}{q_1} = \left(\frac{1}{\epsilon_1} - \frac{1}{2}\right) + \frac{3\kappa r}{16\,\kappa_s^2\, r_1} + \frac{9}{32}\,\kappa_r^2\, I\, q_1 \tag{26}$$

and

$$\frac{e_2 - e_{\omega 2}}{q_1} = \left(\frac{1}{\epsilon_2} - \frac{1}{2}\right)\left(\frac{r_1}{r_2}\right) - \frac{3\kappa_r\, r_1}{16\,\kappa_r^2\, r_2^2} - \frac{9}{32}\left(\frac{r_1}{r_2}\right)^2 \kappa_r^2\, q_1\, I \tag{27}$$

which give for the final flux for concentric cylinders [3]

$$\frac{\sigma(T_1^4 - T_2^4)}{q_1} = \frac{3\kappa L}{4\left(\frac{r_2}{r_1} - 1\right)} \ln\left(\frac{r_2}{r_1}\right) + \left(\frac{1}{\varepsilon_1} - \frac{1}{2}\right) + \frac{r_1}{r_2}\left(\frac{1}{\varepsilon_2} - \frac{1}{2}\right)$$

$$+ \frac{\frac{3}{16}\left(\frac{\kappa_r}{\kappa_s}\right)^2 \left(\frac{r_2}{r_1} - 1\right)}{\kappa_r L \left(\frac{r_2}{r_1}\right)^2} \left[\left(\frac{r_2}{r_1}\right)^2 - 1\right]$$

$$+ \frac{9}{32} \frac{q_1 I}{L^2} \frac{(\kappa_r L)^2}{\left(\frac{r_2}{r_1}\right)^2} \left[\left(\frac{r_2}{r_1}\right)^2 - 1\right] \tag{28}$$

In the limit $\kappa L \to 0$ this reduces to

$$\frac{\sigma(T^4 - T_2^4)}{q} = \frac{1}{\varepsilon_1} + \frac{r_1}{r_2}\left(\frac{1}{\varepsilon_2} - 1\right) \tag{29}$$

which is exactly correct as $r_1 \to r_2$ and which has an accuracy proportional to (r_2/r_1). In the limit $r_2 \to r_1$ the plane slab solution reappears:

$$\frac{\sigma(T_1^4 - T_2^4)}{q_1} = \frac{3\kappa L}{4} + \frac{1}{\varepsilon_1} + \frac{1}{\varepsilon_2} - 1 \tag{30}$$

This cylindrical geometry was studied by Howell and Perlmutter using a NASA Monte Carlo code [6]. Their exact computational results are compared in Fig. 7 with the results of Eq. (28). As r_1 diverges from r_2 the solution given by (28) falls off from the exact Monte Carlo solution below

certain critical values of optical thickness. This is due to the increasing contribution of higher-order terms. However to obtain fast computations that would closely yield the correct results, one could computationally extrapolate the solution to unity after the turning point, as shown by the dotted lines in Figs. 5 and 6.

IV. TEMPERATURE DISCONTINUITIES ON THE BOUNDARIES OF SOURCE REGIONS

Consider two adjacent semi-infinite regions with their common boundary in the x-y plane and with absorption coefficients κ_1 and κ_2 respectively, as in Fig. 8. Applying Eqs. (A6) and (A8) in Appendix A, the net flux over the interface is

$$q_{\nu z} = \frac{dE_2^{above} - dE_1^{below}}{dA}$$

$$= -\frac{1}{4\pi} \sum_{n=0}^{\infty} \sum_{v=0}^{n} \sum_{s=0}^{v} \Omega(nvs) \left[\frac{(-1)^{n-v}}{\kappa_1^n} \left(\frac{\partial^n e_\nu}{\partial z^{n-v}\, \partial y^{v-s}\, \partial x^s} \right)_1 \right.$$

$$\left. - \frac{1}{\kappa_2^n} \left(\frac{\partial^n e_\nu}{\partial z^{n-v}\, \partial y^{v-s}\, \partial x^s} \right)_2 \right] \tag{31}$$

Neglecting terms of higher order than two, Siegel and Howell give the corresponding emissive power jump as [7]

$$e_2 - e_1 = q_{\nu z} + \left\{ - \frac{2}{3}\left[\frac{1}{\kappa_1}\left(\frac{\partial e_\nu}{\partial z}\right)_1 + \frac{1}{\kappa_2}\left(\frac{\partial e_\nu}{\partial z}\right)_2\right] + \frac{1}{2\kappa_1^2}\left(\frac{\partial^2 e_\nu}{\partial z^2} + \frac{1}{2}\frac{\partial^2 e_\nu}{\partial y^2} + \frac{1}{2}\frac{\partial^2 e_\nu}{\partial x^2}\right)_1 - \frac{1}{2\kappa_2^2}\left(\frac{\partial^2 e_\nu}{\partial z^2} + \frac{1}{2}\frac{\partial^2 e_\nu}{\partial y^2} + \frac{1}{2}\frac{\partial^2 e_\nu}{\partial x^2}\right)_2 \right\} \tag{32}$$

Under certain conditions this jump can be nonzero. In particular, as we show below, there is a temperature jump at the boundary of a source region.

First consider the case of two adjacent regions with no sources or sinks. Continuity of flux over the boundary requires that

$$q_z = - \frac{4}{3\kappa_1}\left(\frac{de_\nu}{dz}\right)_1 = - \frac{4}{3\kappa_2}\left(\frac{de_\nu}{dz}\right)_2 \tag{33}$$

But q_z must be constant since no sources are present (i.e., $\frac{dq_z}{dz} = 0$) and therefore $d^2e_\nu/dz^2 = 0$. That is, the second derivatives in (32) vanish and (32) reduces to

$$e_2 - e_1 = q_{\nu z} - \frac{2}{3}\left[\frac{1}{\kappa_1}\left(\frac{\partial e_\nu}{\partial z}\right)_1 + \frac{1}{\kappa_2}\left(\frac{\partial e_\nu}{\partial z}\right)_2\right] = 0 \tag{34}$$

That is, there is no temperature jump over a stagnant boundary.

On the other hand, consider the presence of sources in the two regions and define the sources by the flux gradients

$$S_i = \left(\frac{dq}{dz}\right)_i = -\frac{4}{3\kappa_i}\left(\frac{\partial^2 e_\nu}{\partial z^2}\right)_i \tag{35}$$

In this case the emissive power jump given by (32) becomes

$$e_2 - e_1 = q_{\nu z} - \frac{2}{3}\left[\frac{1}{\kappa_1}\left(\frac{\partial e_\nu}{\partial z}\right)_1 + \frac{1}{\kappa_2}\left(\frac{\partial e_\nu}{\partial z}\right)_2\right] + \frac{1}{2}\left[\frac{1}{\kappa_1^2}\left(\frac{\partial^2 e_\nu}{\partial z^2}\right)_1 - \frac{1}{\kappa_2^2}\left(\frac{\partial^2 e_\nu}{\partial z^2}\right)_2\right] \tag{36}$$

But since (33) is still valid on either side of the boundary this becomes

$$e_2 - e_1 = q_{\nu z} - \frac{2}{3}\left[\frac{1}{\kappa_1}\left(\frac{3\kappa_1}{4} q_z\right) + \frac{1}{\kappa_2}\left(\frac{3\kappa_2}{4} q_z\right)\right] + \frac{1}{2}\left[\frac{1}{\kappa_1^2}\left(-\frac{3\kappa_1}{4} S_1\right) - \frac{1}{\kappa_2^2}\left(-\frac{3\kappa_2}{4} S_2\right)\right] \tag{37}$$

which reduces to

$$e_2 - e_1 = \frac{3}{8}\left(\frac{S_1}{\kappa_1} - \frac{S_2}{\kappa_2}\right) \tag{38}$$

Thus at source boundaries there is a temperature jump. This fact was noted in 1967 by Howell [8] in his more exact calculations in terms of integral equations, which yield a factor of $\frac{1}{4}$ instead of the $\frac{3}{8}$ above.

V. CONCLUSION

Recent developments in the literature of thermal radiation transfer have indicated the importance of temperature jump boundary conditions at walls

and on source boundaries in general. In diffusion approximations, either analytic or from computer codes, these boundary conditions rightfully belong in the solution and indeed at low optical thicknesses they can have a drastic influence on the amount of radiative flux that is transferred from one region to another.

The equations presented in this paper involve several assumptions and approximations that should be explored. No attempt has been made to suggest how the wall emissivity ε might be calculated, although for most high-temperature cases a blackbody assumption ($\varepsilon = 1$) is reasonable. The jump boundary conditions need to be derived for nongrey scattering media. Non-isotropic fluxes should be considered more explicitly. Analytic solutions can be derived for geometries other than those considered here. The effects of large variations in the absorption coefficient, such as are often encountered in real materials, need to be explored. Thus there is a great deal of interesting work that can be done to extend this theory. Some of it already exists in the numerous papers on the subject that have appeared in the last decade [3, 6, 7, 8, 9, 10, 11, 12].

In spite of all these complications, the basic idea remains clear: that the application of temperature jump boundary conditions, even in crude approximation, can correct a pure diffusion solution at low optical thicknesses to give a solution that is much closer to the correct solution. Their application markedly extends the range of validity of the diffusion approximation.

APPENDIX A: THE GENERAL EQUATIONS OF ENERGY FLUX AND TEMPERATURE JUMP IN THE DIFFUSION APPROXIMATION

We present here the derivation of Deissler [3] for the temperature jump boundary conditions in the photon diffusion approximation. Consider radiation streaming through an area element dA in a transparent medium at point (x_0, y_0, z_0) as in Fig. 3. The radiation is emitted from volume element dV at (x, y, z). The spectral emissive power e_ν (e.g., ergs/cm^2 sec) is defined by Planck's equation written in a different form:

$$e_\nu = \frac{2\pi h\nu^3}{c^2 \exp\left[h\nu\, \sigma^{1/4} k^{-1} e_g^{-1/4}\right] - 1} \tag{A1}$$

where ν is the frequency, c is the speed of light, h is Planck's constant, σ is the Stefan-Boltzmann constant, k is the Boltzmann constant, and $e_g = \sigma T^4$. Expand e_ν in a Taylor series about $(x_0\ y_0\ z_0)$:

$$e_\nu = \sum_{n=0}^{\infty} \frac{1}{n!} \left[(z - z_0) \left(\frac{\partial}{\partial z}\right)_0 + (y - y_0) \left(\frac{\partial}{\partial y}\right)_0 + (x - x_0) \left(\frac{\partial}{\partial x}\right)_0 \right]^n e_\nu \quad . \tag{A2}$$

Applying the binomial theorem twice to the factor in brackets,

$$e_\nu = \sum_{n=0}^{\infty} \sum_{v=0}^{n} \sum_{s=0}^{v} \frac{(z - z_0)^{n-v} (y - y_0)^{v-s} (x - x_0)^s}{(n - v)!\ (v - s)!\ s!} \cdot \left(\frac{\partial^n e_\nu}{\partial z^{n-v}\ \partial y^{v-s}\ \partial x^s} \right)_0 \tag{A3}$$

Let κ_ν represent the spectral absorption coefficient of the material in the transparent medium. The opacity μ is then $\mu = 1/\kappa\rho$ (e.g., cm^2/gm). From Bouguer's law the emitted intensity diminishes as $e^{-\kappa_\nu r}$, and the flux from dV at frequency ν which passes through the thin element dA is then

$$dE_\nu = 4\kappa_\nu e_\nu \, dV \frac{d\omega}{4\pi} e^{-\kappa_\nu r} . \tag{A4}$$

(In using Bouguer's law the assumption has been made that κ_ν is effectively uniform over a mean free path. This assumption will not always be justified.)

The solid angle is $d_\omega = dA \cos\theta/r^2$ and the volume element is $dV = r^2 \sin\theta dr d\theta d\phi$. In spherical coordinates

$$x - x_0 = r \sin\theta \cos\phi$$
$$y - y_0 = r \sin\theta \sin\phi$$
$$z - z_0 = r \cos\phi$$

Thus the energy flux from above dA ($0 < \theta < \pi/2$) is

$$dE_{\nu 1} = \frac{\kappa_\nu dA}{\pi} \sum_{n=0}^{\infty} \sum_{v=0}^{n} \sum_{s=0}^{v} \frac{1}{(n-v)!\,(v-s)!\,s!} \cdot \left(\frac{\partial^n e_\nu}{\partial z^{n-v} \, \partial y^{v-s} \, \partial x^s} \right)_0 \cdot \int_0^{\pi/2} \int_0^{2\pi} \int_0^{\infty} (r\cos\theta)^{n-v} (r\sin\theta\sin\phi)^{v-s} \cdot (r\sin\theta\cos\phi)^s \cos\theta \sin\theta \, e^{-\kappa_\nu r} \, dr d\phi d\theta , \tag{A5}$$

The solution to this integral is

$$(A6) \qquad dE_\nu = \frac{dA}{4\pi} \sum_{n=0}^{\infty} \sum_{v=0}^{n} \sum_{s=0}^{n} \Omega(n,v,s) \; \frac{1}{\kappa_\nu^n} \left(\frac{\partial^n e_\nu}{\partial z^{n-v} \; \partial y^{v-s} \; \partial x^s} \right)_0$$

where

$$(A7) \qquad \Omega(nvs) = \frac{\left[1 + (-1)^{v-s}\right]\left[1 + (-1)^s\right] n! \left(\Gamma \frac{n - v + 2}{2}\right)\Gamma\left(\frac{v - s + 1}{2}\right)\Gamma\left(\frac{s + 1}{2}\right)}{(n - v)!\ (v - s)!\ s!\ \Gamma\left(\frac{n + 4}{2}\right)}$$

Similarly the energy flux from below dA ($\pi/2 < \theta < \pi$) is given by

$$(A8) \qquad dE_{\nu 2} = \frac{dA}{4\pi} \sum_{n=0}^{\infty} \sum_{v=0}^{n} \sum_{s=0}^{v} (-1)^{n-v} \; \Omega(nvs) \; \frac{1}{\kappa_\nu^n} \cdot \left(\frac{\partial^n e_\nu}{\partial z^{n-v} \; \partial y^{v-s} \; \partial x^s} \right)_0$$

The net flux in the z direction is then

$$(A9) \qquad q_{\nu z} = \frac{dE_{\nu 2} - dE_{\nu 1}}{dA}$$

$$= - \frac{1}{4\pi} \sum_{n=0}^{\infty} \sum_{v=0}^{n} \sum_{s=0}^{v} \left[1 - (-1)^{n-v}\right] \Omega(nvs) \; \frac{1}{\kappa^n} \cdot \left(\frac{\partial^n e_\nu}{\partial z^{n-v} \; \partial y^{v-s} \; \partial x^s} \right)$$

Next the jump boundary conditions will be derived for a grey wall (i.e., one whose absorption and emission coefficients are independent of frequency) which is below the area dA. The energy coming from the wall and passing through dA is made up of the radiation emitted by the wall

and the radiation originating in the transparent medium and reflected by the wall. From Kirchhoff's law

$$(A10) \qquad dE_{\nu 2} = \varepsilon e_{\nu b}\, dA + (1 - \varepsilon)\, dE_{\nu 1} \quad ,$$

where ε is the wall emissivity (i.e., the ratio of the actual emitted energy of the wall to the emitted energy of the wall if it were a black-body) and $e_{\nu b}$ is the emissive power for a black wall. Solving this equation for $e_{\nu b}$,

$$(A11) \qquad e_{\nu b} = \frac{1}{\varepsilon}\left(\frac{dE_{\nu 2} - dE_{\nu 1}}{dA}\right) + \frac{dE_{\nu 1}}{dA}$$

$$= \left(\frac{1}{\varepsilon} - \frac{1}{2}\right) q_{\nu z} + \frac{1}{2}\, q_{\nu z} + \frac{dE_{\nu 1}}{dA}$$

Substituting (A6) and (A9) into (A11) and removing the term from n = 0 gives the jump:

$$(A12) \qquad (e_{\nu b} - e_{\nu 0})_{below} = \left(\frac{1}{\varepsilon} - \frac{1}{2}\right) q_{\nu z 0} + \frac{1}{8\pi} \sum_{n=1}^{\infty} \sum_{v=0}^{n} \sum_{s=0}^{v}$$

$$\cdot\, [1 + (-1)^{n-v}]\, \Omega(nvs)\, \frac{1}{\kappa_\nu^n} \left(\frac{\partial^n e_\nu}{\partial z^{n-v}\, \partial y^{v-s}\, \partial x^s}\right)_0$$

Similarly if the wall is above rather than below dA,

$$(A13) \qquad (e_{\nu 0} - e_{\nu b})_{above} = \left(\frac{1}{\varepsilon} - \frac{1}{2}\right) q_{\nu z 0} - \frac{1}{8\pi} \sum_{n=1}^{\infty} \sum_{v=0}^{n} \sum_{s=0}^{v}$$

$$\cdot\, [1 + (-1)^{n-v}]\, \Omega(nvs)\, \frac{1}{\kappa_\nu^n} \left(\frac{\partial^n e_\nu}{\partial z^{n-v}\, \partial y^{v-s}\, \partial x^s}\right)_0$$

Thus Eqs. (A7), (A9), (A12), and (A13) give the general expressions for the energy flux in the medium and for the energy jumps at the walls.

If terms of higher order than second are neglected, Eqs. (A7) and and (A9) reduce to the usual Rosseland steady state diffusion equation

$$(A14) \qquad q_{\nu z} = - \frac{4}{3\kappa\nu} \frac{\partial e_\nu}{\partial z}$$

but now it is constrained by the jump boundary conditions

$$(A15) \qquad e_{\nu b} - e_{\nu 0} = \left(\frac{1}{\varepsilon} - \frac{1}{2}\right) q_{\nu z 0} + \frac{1}{2\kappa_\nu^2}\left(\frac{\partial^2 e_\nu}{\partial z^2}\right)_0 + \frac{1}{4\kappa_\nu^2}\left(\frac{\partial^2 e_\nu}{\partial y^2}\right)_0 + \frac{1}{4\kappa_\nu^2}\left(\frac{\partial^2 e_\nu}{\partial x^2}\right)_0$$

for a wall below the transparent medium and

$$(A16) \qquad e_{\nu 0} - e_{\nu b} = \left(\frac{1}{\varepsilon} - \frac{1}{2}\right) q_{\nu z 0} - \frac{1}{2\kappa_\nu^2}\left(\frac{\partial^2 e_\nu}{\partial z^2}\right)_0 - \frac{1}{4\kappa_\nu^2}\left(\frac{\partial^2 e_\nu}{\partial y^2}\right)_0 - \frac{1}{4\kappa_\nu^2}\left(\frac{\partial^2 e_\nu}{\partial x^2}\right)_0$$

for a wall above the medium.

These equations apply to a single frequency ν. By using Eq. (A1) these equations can be integrated over ν to obtain equations for the total one-group radiative flux and the total emissive power. Then the opacity becomes the Rosseland mean κ_r and Eqs. (A7)-(A13) become

$$(A17) \qquad q_z = - \frac{4}{3\kappa_r} \frac{\partial e_g}{\partial z}$$

where $e_g = \sigma T^4$ in the transparent medium, and

$$(A18) \qquad \pm (e_b - e_{g0}) = \left(\frac{1}{\varepsilon} - \frac{1}{2}\right) q_{z0} \pm \frac{1}{2\kappa_s^2}\left(\frac{\partial^2 e_g}{\partial z^2}\right)_0 \pm \frac{I}{2}\left(\frac{\partial e_g}{\partial z}\right)_0^2$$
$$\pm \frac{1}{4\kappa_s^2}\left(\frac{\partial^2 e_g}{\partial y^2}\right)_0 \pm \frac{I}{4}\left(\frac{\partial e_g}{\partial y}\right)_0^2 \pm \frac{1}{4\kappa_s^2} \pm \left(\frac{\partial^2 e_g}{\partial x^2}\right)_0 \pm \frac{I}{4}\left(\frac{\partial e_g}{\partial x}\right)_0^2$$

where the + sign is for a wall <u>below</u> the transparent medium, the - sign is for a wall <u>above</u> the medium, the subscript "0" implies evaluation in the transparent medium infinitesimally close to the wall, and

$$(A19) \qquad \frac{1}{\kappa_r} = \int_0^\infty \frac{1}{\kappa_\nu} \frac{\partial e_\nu}{\partial e_g} \, d\nu \; ;$$

$$(A20) \qquad \frac{1}{\kappa_s^2} \int_0^\infty \frac{1}{\kappa_\nu^2} \frac{\partial e_\nu}{\partial e_g} \, d\nu \; ;$$

$$(A21) \qquad I = \int_0^\infty \frac{1}{\kappa_\nu^2} \frac{\partial^2 e_\nu}{\partial e_g^2} \, d\nu \; .$$

The derivatives of e_ν with respect to e_g are obtained from Eq. (A1).

For a grey gas, κ_ν is independent of ν and (A21) becomes

$$(A22) \qquad I = \frac{1}{\kappa_\nu^2} \frac{\partial^2}{\partial e_g^2} \int_0^\infty e_\nu d\nu = \frac{1}{\kappa_\nu^2} \frac{\partial^2 e_g}{\partial e_g^2} = 0 \; .$$

For a nongrey gas it is necessary to know κ_ν as a function of ν and e_g in order to calculate κ_r, κ_s, and I.

REFERENCES

1. G. N. Patterson, Molecular Flow of Gases, Wiley, (1956).

2. R. A. Millikan, Phys. Rev. 21, 217 (1923).

3. R. G. Deissler, J. Heat Transfer 86, 240 (1964).

4. J. C. Maxwell, Scientific Papers 2, 705.

5. S. Rosseland, Astrophysik auf Atom-Theoretischer Grundlage, Julius Springer Verlag, Berlin, (1931).

6. M. Perlmutter and J. R. Howell, J. Heat Transfer 86, 169 (1964).

7. R. Siegel and J. R. Howell, Thermal Radiation Heat Transfer, McGraw-Hill, 478, (1972).

8. J. R. Howell, NASA-TN-D-3614, (1966).

9. D. B. Olfe and S. S. Penner, J. Quant. Spect. Rad. Transf. 4, 229 (1964).

10. R. F. Probstein, AIAAJ 1, 1202 (1963).

11. M. A. Heaslet and R. F. Warming, Int. J. Heat Mass Transfer 8, 979 (1965).

12. J. R. Howell, Int. J. Heat Mass Transfer 10, 401 (1967).

13. M. L. Alme and J. R. Wilson, Astrophysical Journal 194, p. 147 (1974).

14. D. S. Kershaw, Lawrence Livermore Laboratory internal report UCRL-78378.

FIGURE CAPTIONS

Figure 1. An illustration of the temperature jump at a wall at temperature T_ω caused by diffuse reflection of molecules from a gas at temperature T_g and mean free path λ flowing along the wall.

Figure 2. Schematic representation of how the slip velocity or alternatively the temperature jump at a wall varies with Knudsen number $K_n = \lambda/L$, indicating roughly the transition regime between free molecular flow and no-slip flow where temperature jump is important.

Figure 3. Schematic of the geometry used for deriving the diffusion equation with temperature jump boundary conditions.

Figure 4. Illustration of the three geometries for which explicit solutions to the diffusion equation with temperature jump boundary conditions have been obtained. In each case the region between the walls is filled with an absorbing material of opacity $1/\kappa\rho$.

Figure 5. Analytic solutions for the normalized flux between two infinite parallel blackbody source walls as a function of optical thickness κL of the material between the walls. The upper curve gives the diffusion solution with no boundary

conditions and the lower curve gives the solution with temperature jump boundary conditions. The latter solution is exact to all orders.

Figure 6. Analytic solutions for the normalized flux between two concentric spherical blackbody source walls as a function of optical thickness of the material between the walls and in terms of the parameter r_1/r_2. The solid curves are the solutions of the diffusion equation with temperature jump boundary conditions accurate to second order. The accuracy of these curves is good until they turn over; beyond the turning point an extrapolation such as the dashed curve is very close to the analytic solution given by Monte Carlo calculations. For comparison, the dot-dash curve gives the pure diffusion solution for $r_1/r_2 = 0.75$ and no boundary conditions.

Figure 7. Analytic solutions for the normalized flux between two concentric cylindrical blackbody source walls as a function of optical thickness of the material between the walls and in terms of the parameter r_1/r_2. The solid curves are solutions of the diffusion equation with temperature jump boundary conditions accurate to second order. The dashed curves are Monte Carlo results from the NASA research of Howell and Perlmutter [6].

Figure 8. Illustration of the temperature jump at the boundary between two absorbing regions one or both of which contains a source or a sink.

Figure 9. Temperature distributions between two parallel radiating slabs as a function of optical thickness of the material between.

Figure 10. Temperature jump at the walls of two parallel radiating slabs as a function of optical thickness of the material between. Note that while ΔT^4 is the same at either wall, the actual temperature jump ΔT is not.

Figure 11. Temperature distributions between concentric radiating spheres as a function of optical thickness κL for the case $r_1/r_2 = 0.75$.

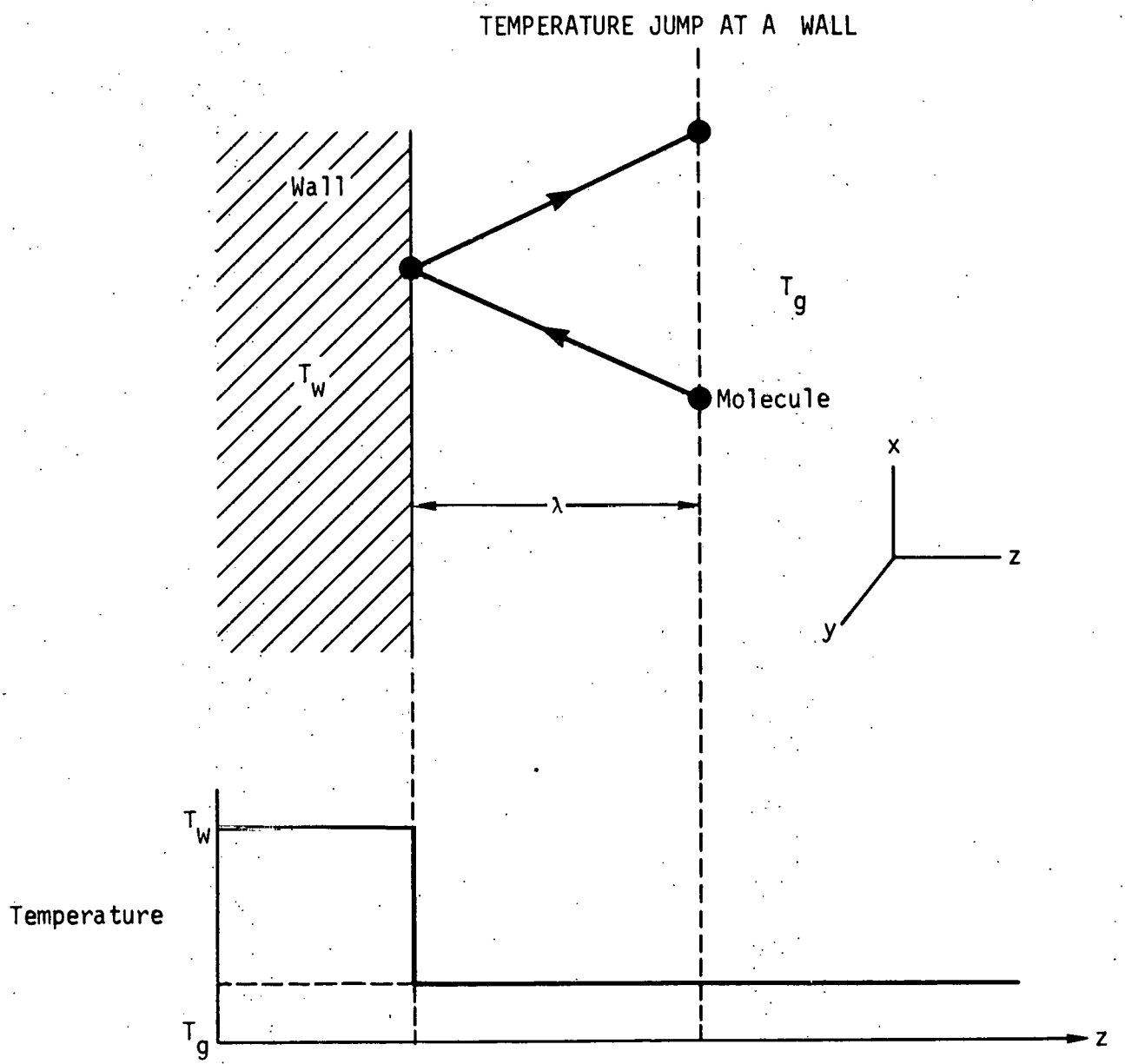
TEMPERATURE JUMP AT A WALL
Wall
T_w
T_g
Molecule
λ
x
z
y
Temperature
T_w
T_g
z

Figure 1

VARIATION OF TEMPERATURE JUMP WITH KNUDSEN NUMBER

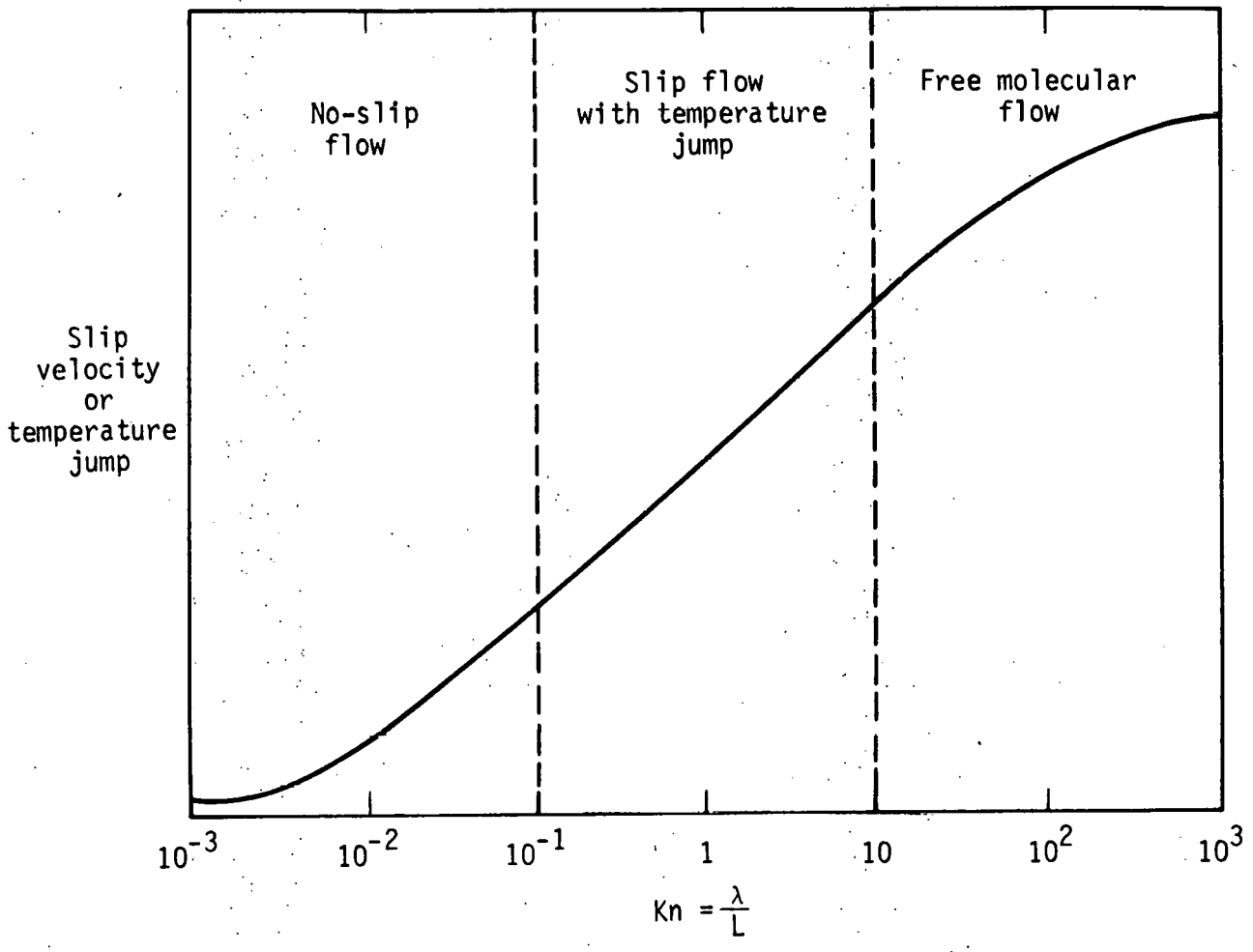

Figure 2

GEOMETRY FOR DIFFUSION EQUATIONS

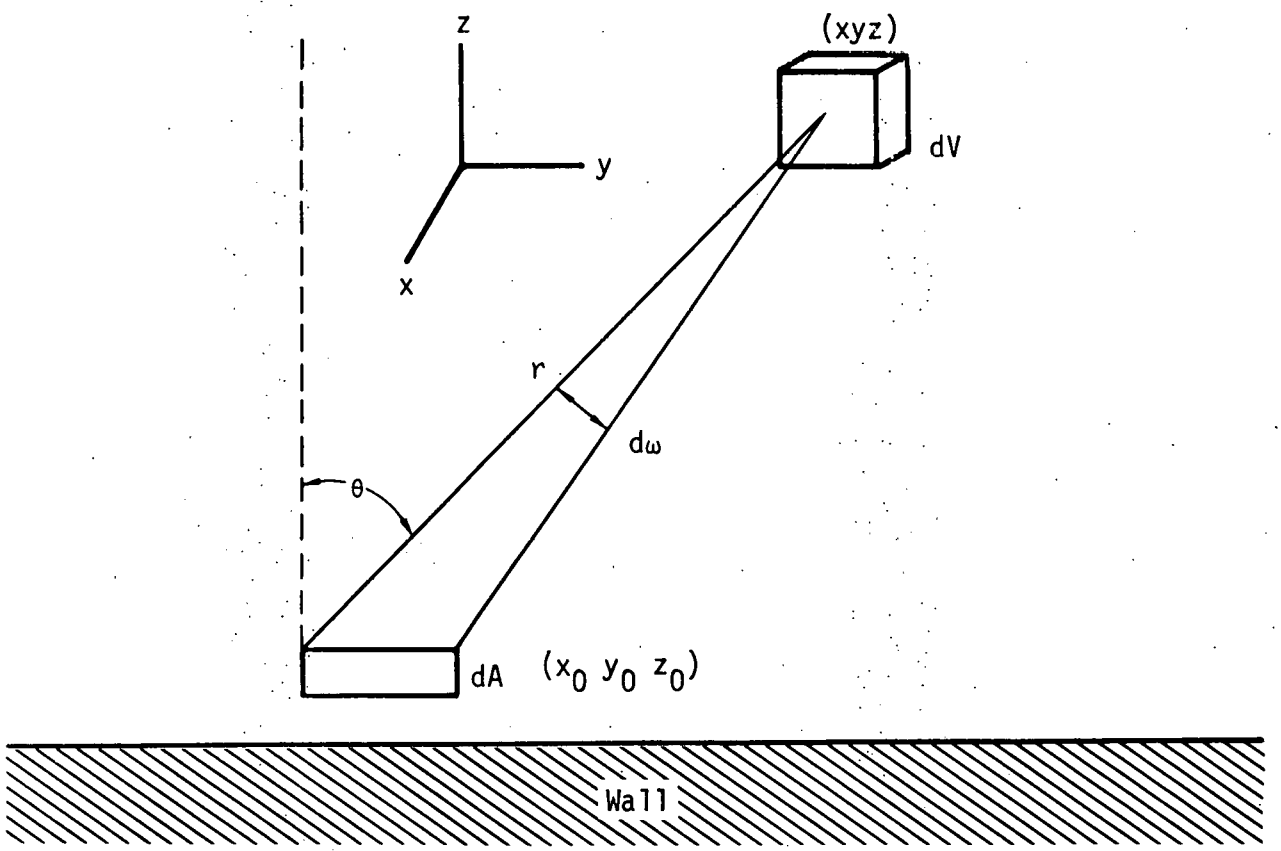

Figure 3

SPECIFIC GEOMETRIES FOR CALCULATIONS

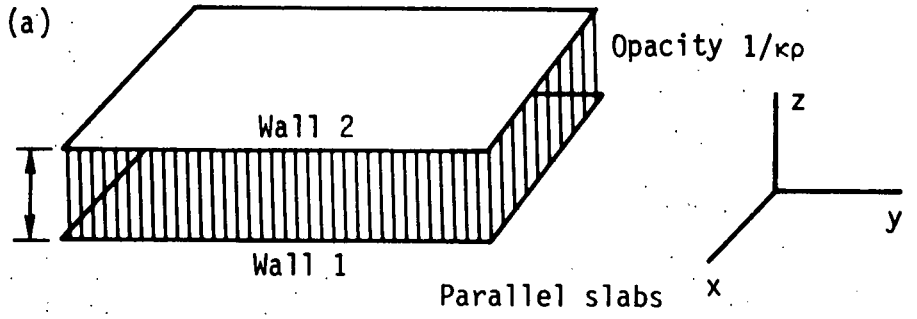

Parallel slabs

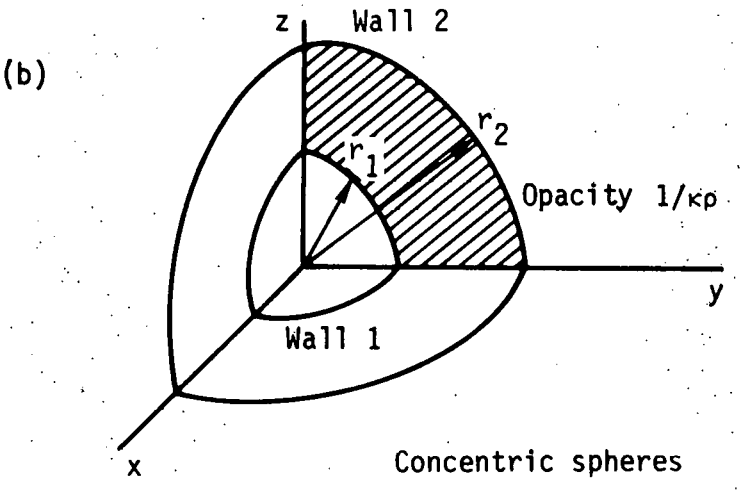

Concentric spheres

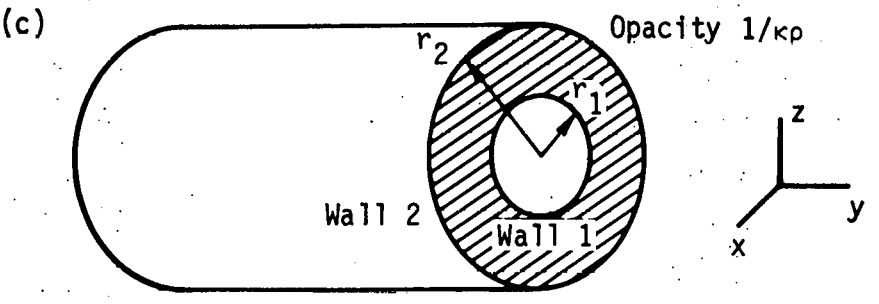

Concentric cylinders

Figure 4

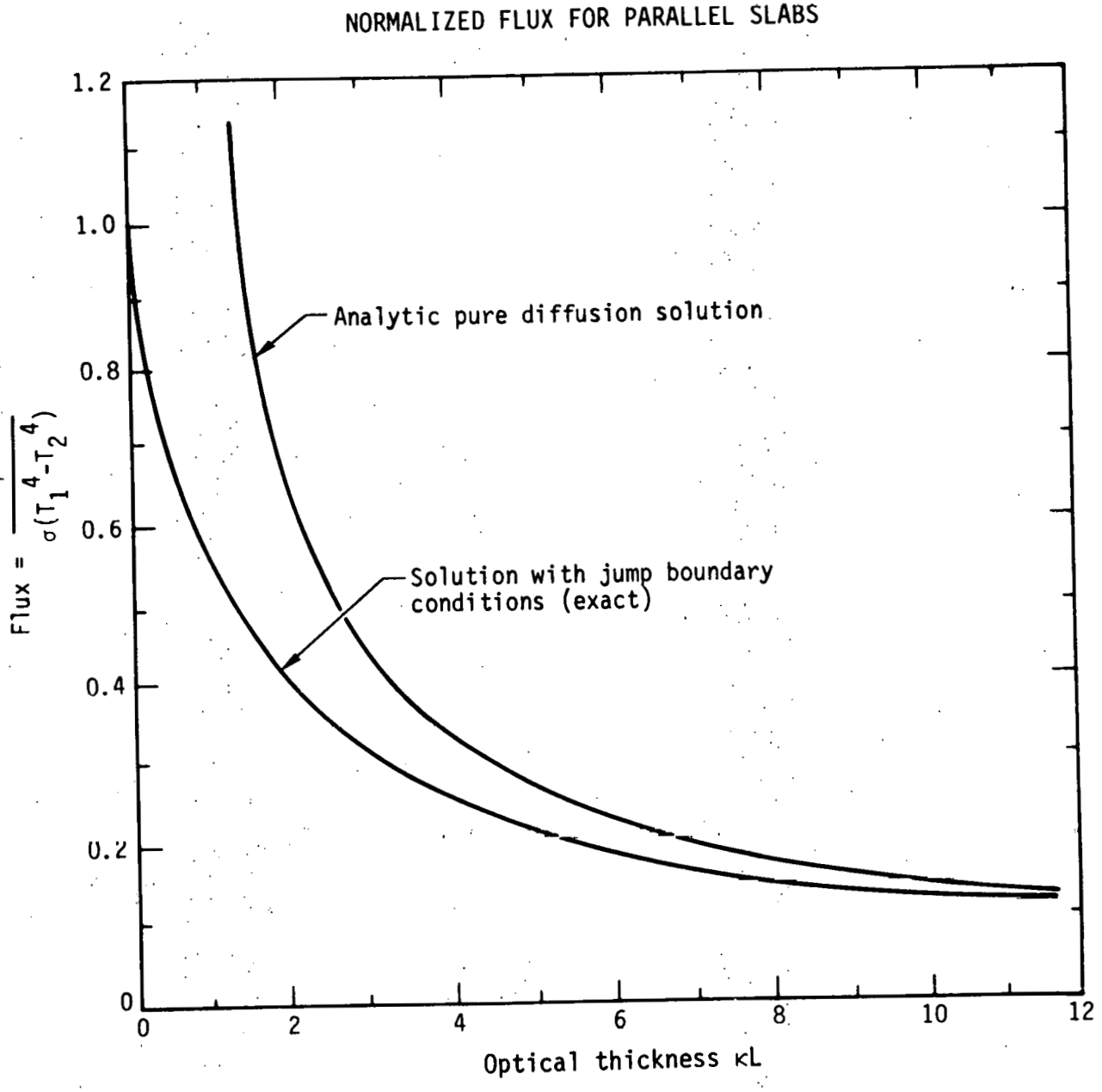
NORMALIZED FLUX FOR PARALLEL SLABS
Flux = $\frac{q}{\sigma(T_1^4 - T_2^4)}$
1.2
1.0
0.8
0.6
0.4
0.2
0
0
2
4
6
8
10
12
Optical thickness κL
Analytic pure diffusion solution
Solution with jump boundary conditions (exact)

Figure 5

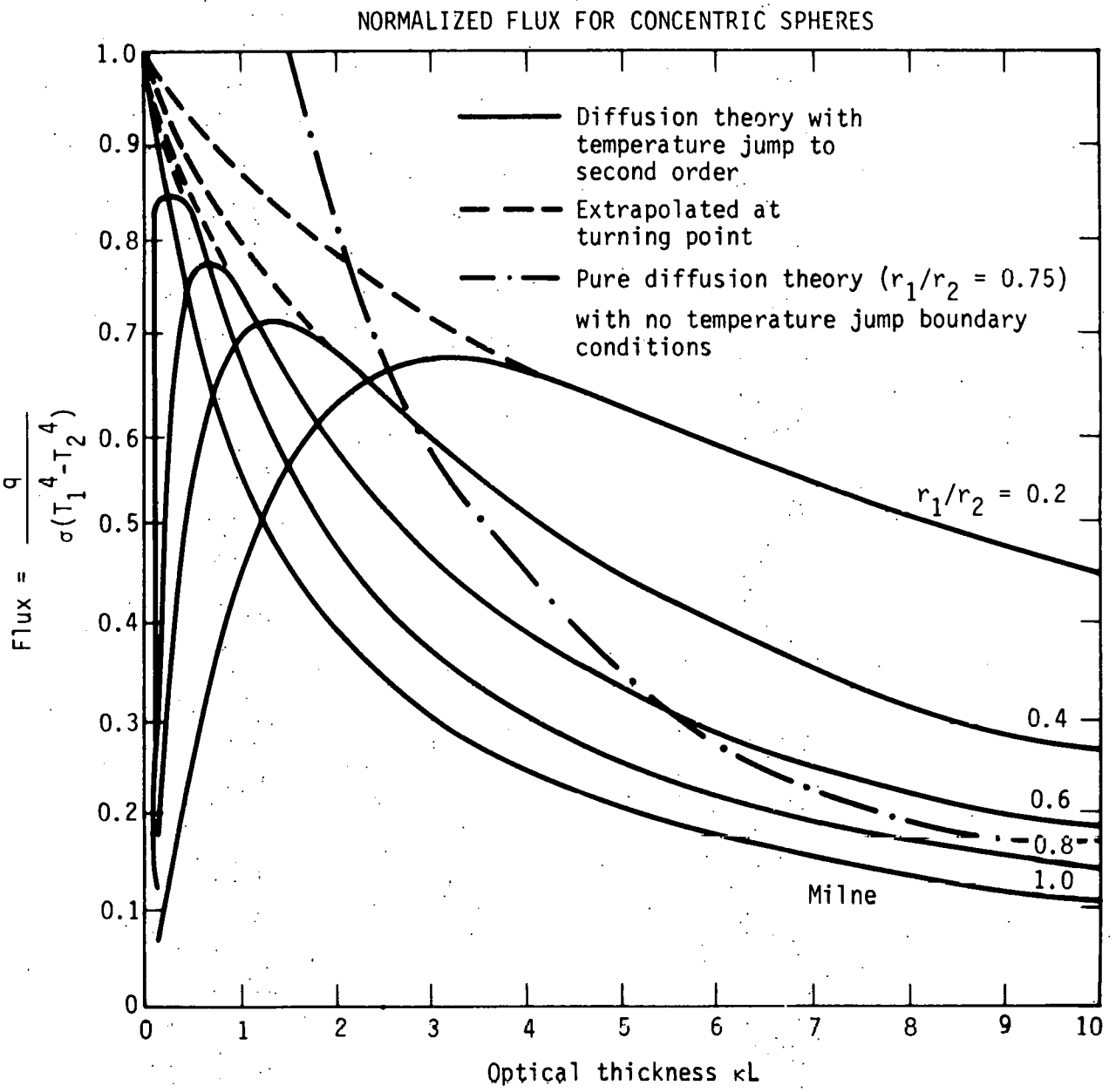
NORMALIZED FLUX FOR CONCENTRIC SPHERES
Diffusion theory with temperature jump to second order
Extrapolated at turning point
Pure diffusion theory (r_1/r_2 = 0.75) with no temperature jump boundary conditions
r_1/r_2 = 0.2
0.4
0.6
0.8
1.0
Milne
Flux = $\frac{q}{\sigma(T_1^4-T_2^4)}$
Optical thickness κL
0
0.1
0.2
0.3
0.4
0.5
0.6
0.7
0.8
0.9
1.0
0
1
2
3
4
5
6
7
8
9
10

Figure 6

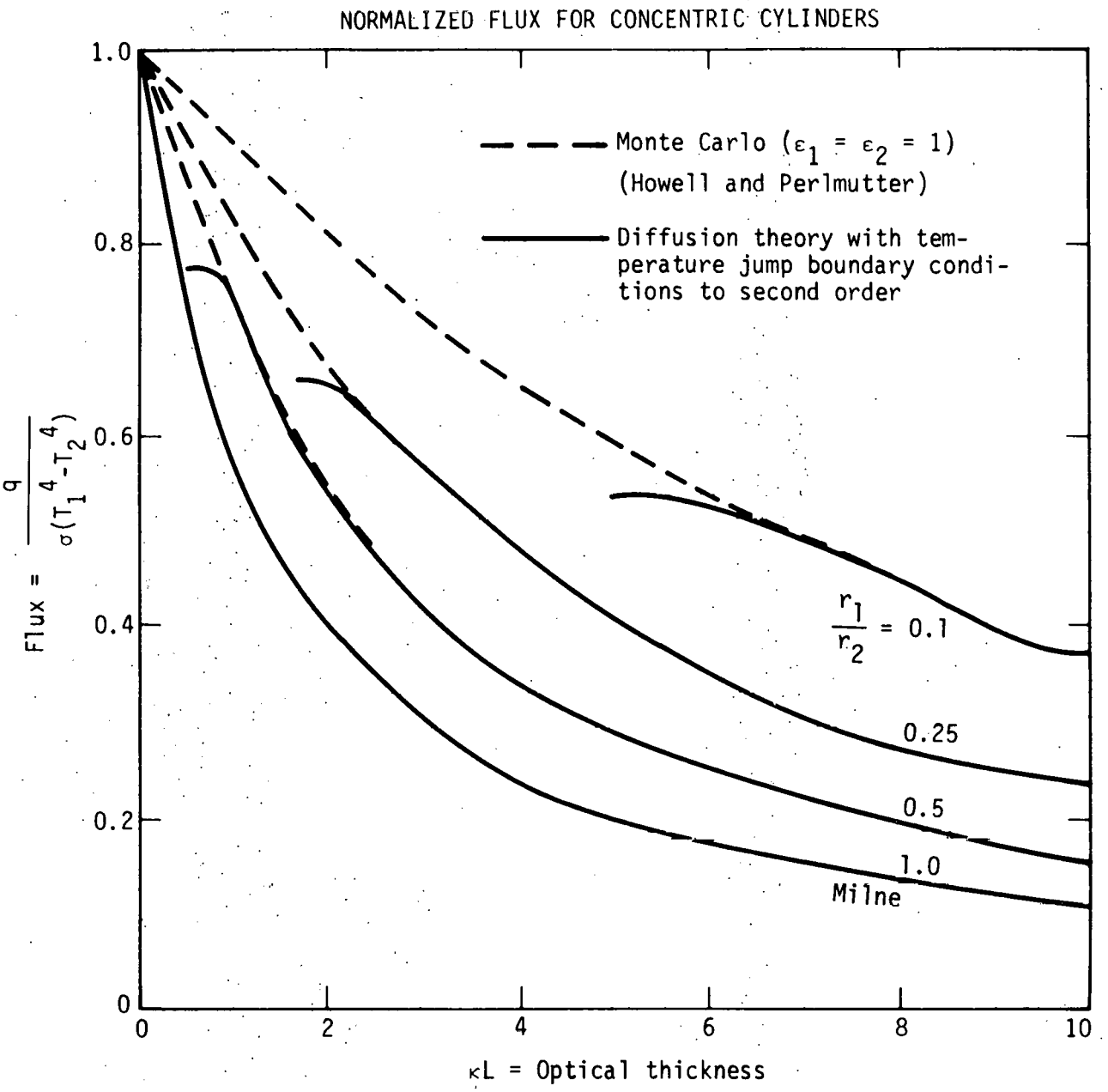
NORMALIZED FLUX FOR CONCENTRIC CYLINDERS
Monte Carlo ($\varepsilon_1 = \varepsilon_2 = 1$)
(Howell and Perlmutter)
Diffusion theory with temperature jump boundary conditions to second order
$\frac{r_1}{r_2}$ = 0.1
0.25
0.5
1.0
Milne
Flux = $\frac{q}{\sigma(T_1^4 - T_2^4)}$
1.0
0.8
0.6
0.4
0.2
0
0
2
4
6
8
10
κL = Optical thickness

Figure 7

TEMPERATURE JUMP AT A SOURCE BOUNDARY

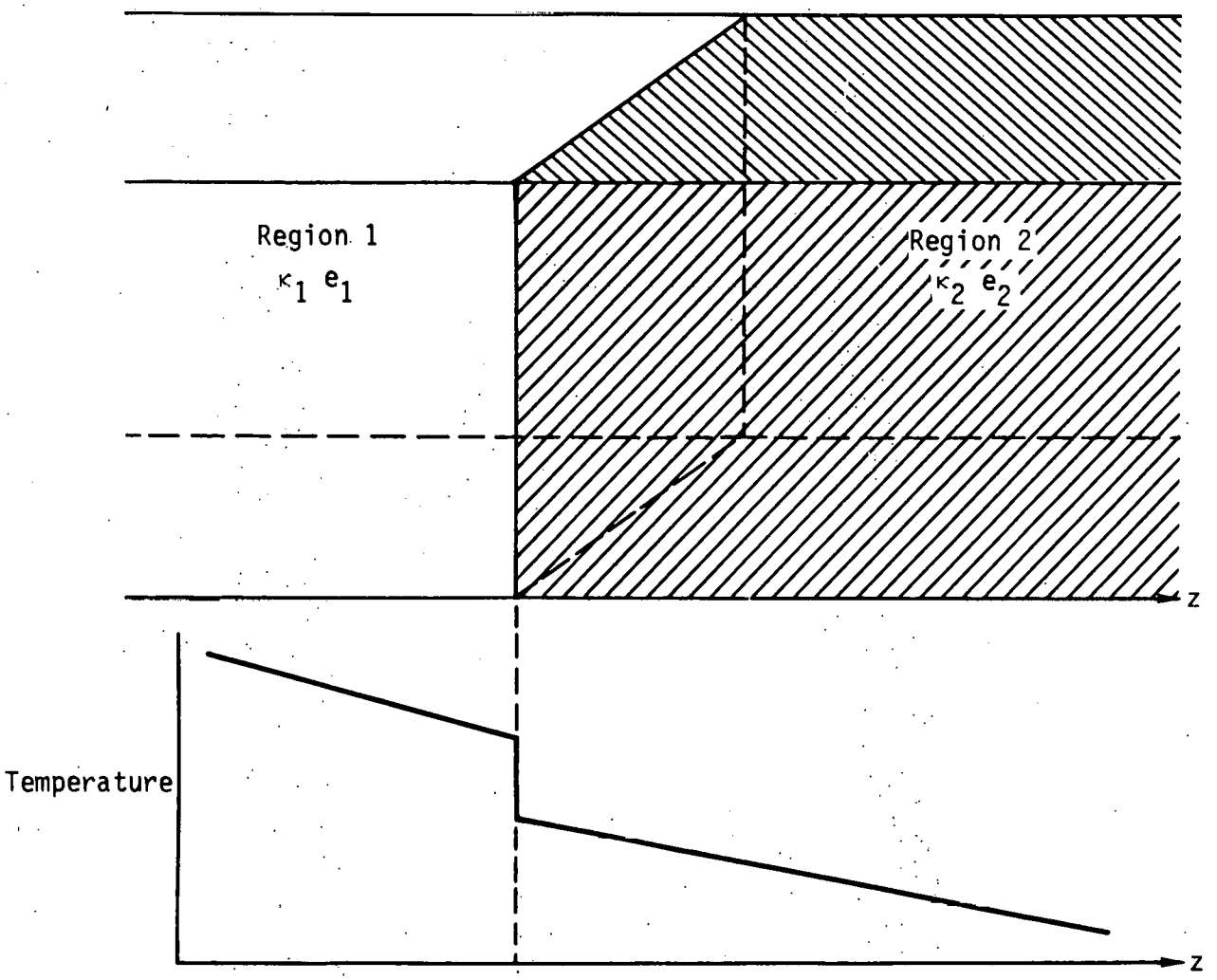

Figure 8

TEMPERATURE DISTRIBUTION FOR PARALLEL SLABS

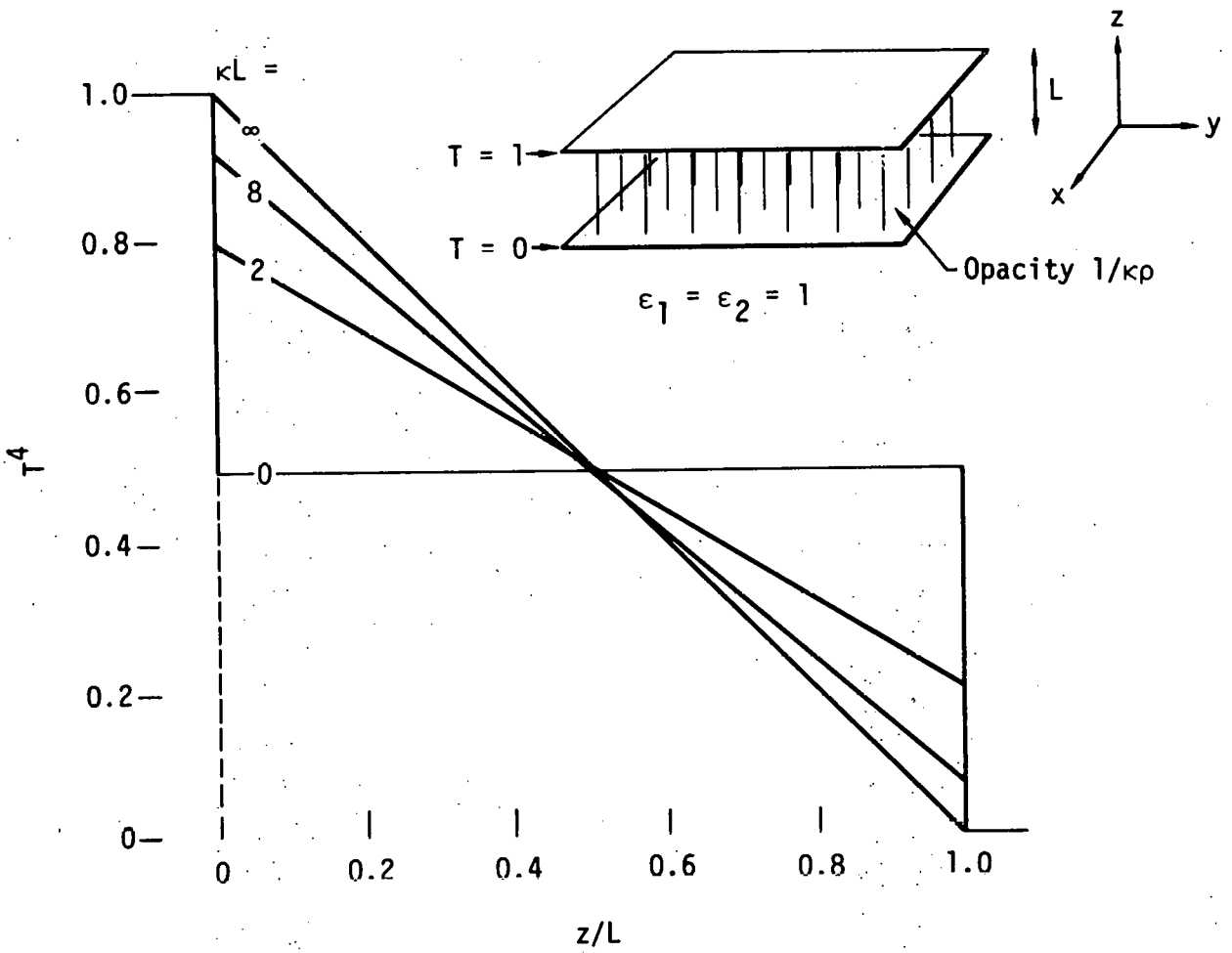

Figure 9

TEMPERATURE JUMP VS OPTICAL THICKNESS
FOR PARALLEL SLABS
(T_i = 1.0 T_2 = 0 $\varepsilon_1 = \varepsilon_2$ = 1.0)

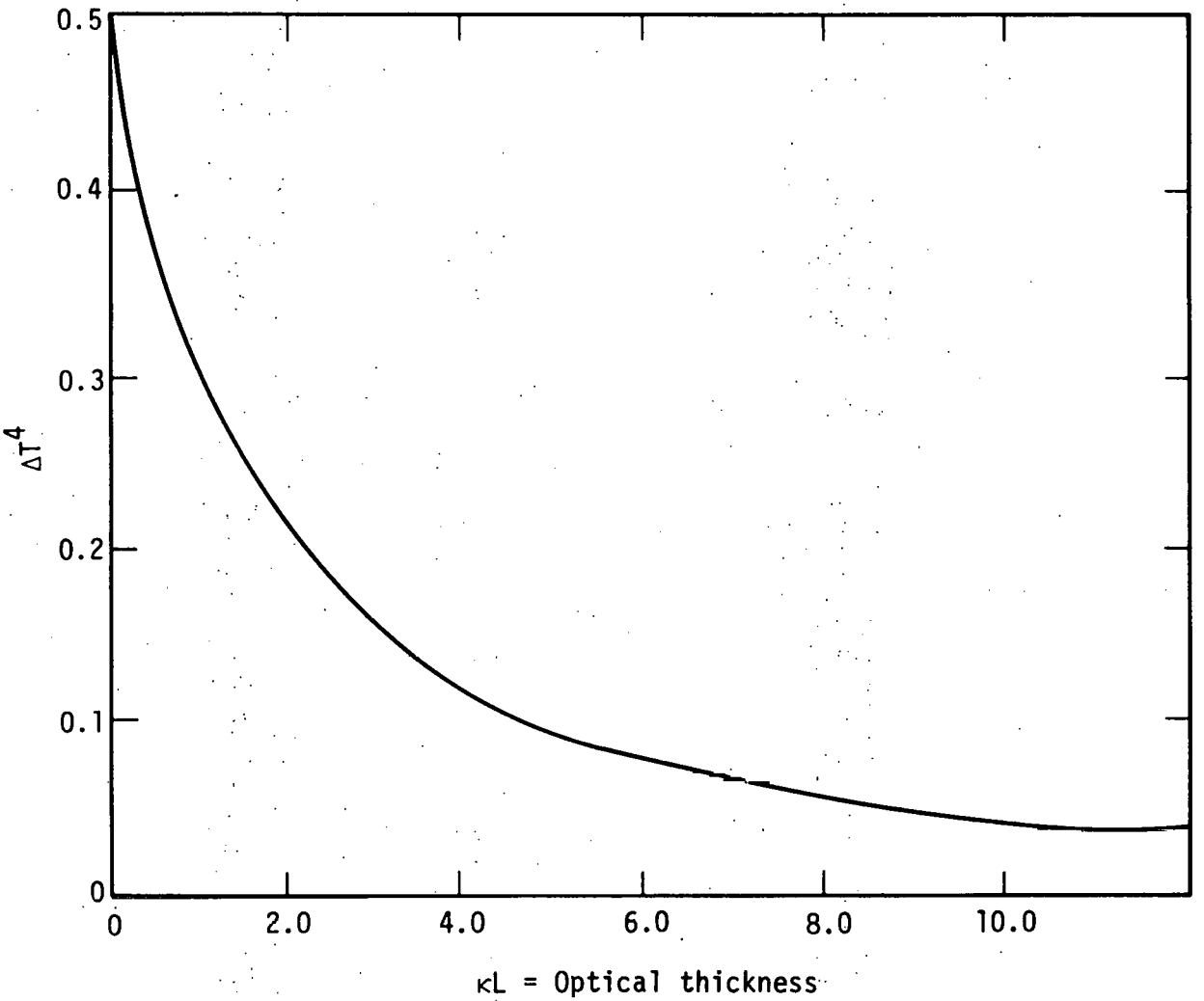

Figure 10

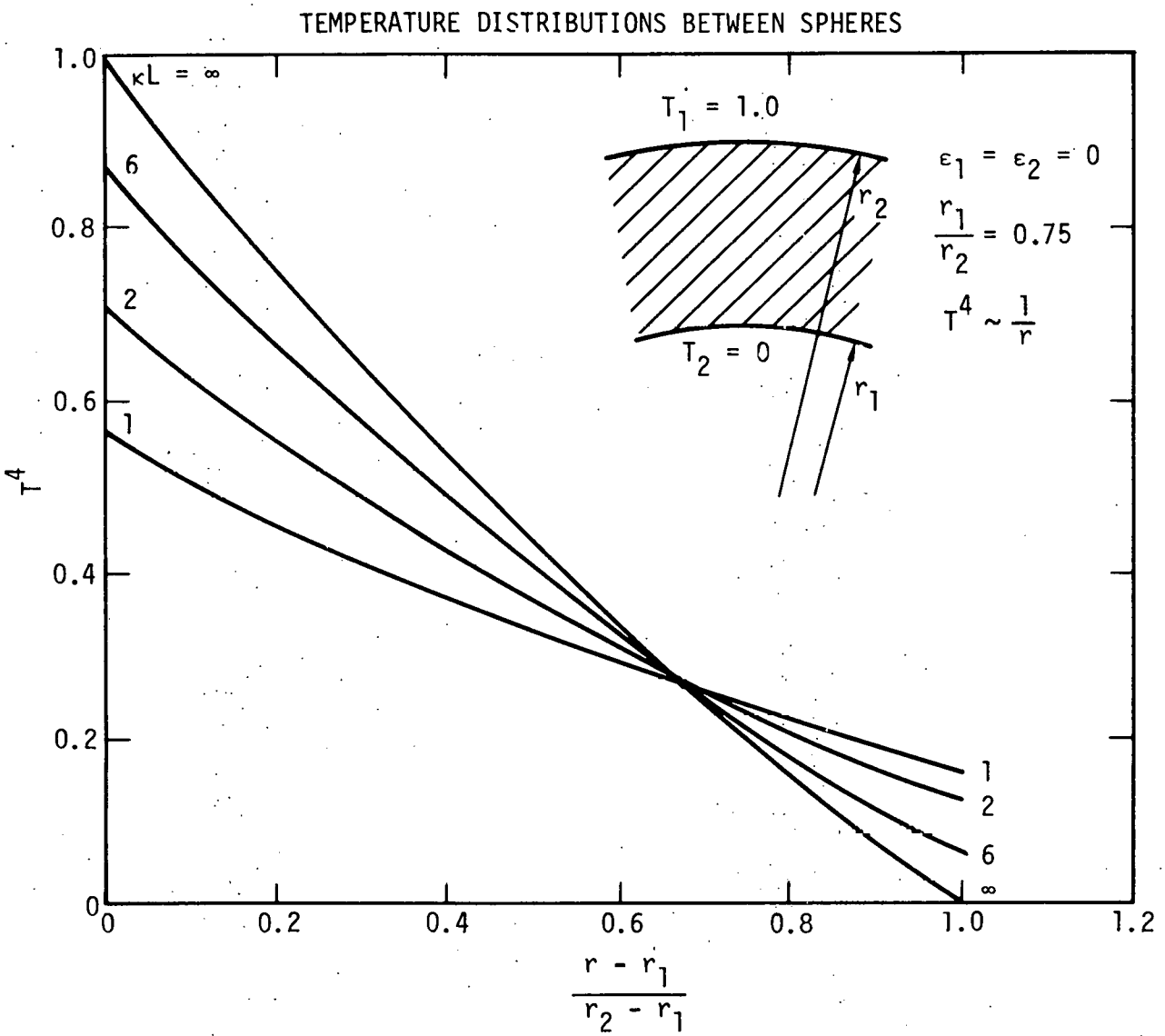
TEMPERATURE DISTRIBUTIONS BETWEEN SPHERES
κL = ∞
6
2
1
$T_1 = 1.0$
$T_2 = 0$
r_2
r_1
$\varepsilon_1 = \varepsilon_2 = 0$
$\frac{r_1}{r_2} = 0.75$
$T^4 \sim \frac{1}{r}$
T^4
$\frac{r - r_1}{r_2 - r_1}$
0
0.2
0.4
0.6
0.8
1.0
1.2
1
2
6
∞

Figure 11

Printed in the United States of America
Available from
National Technical Information Service
U.S. Department of Commerce
5285 Port Royal Road
Springfield, VA 22161
Price: Printed Copy $; Microfiche $3.00

Page Range	Domestic Price	Page Range	Domestic Price
001–025	$ 3.50	326–350	10.00
026–050	4.00	351–375	10.50
051–075	4.50	376–400	10.75
076–100	5.00	401–425	11.00
101–125	5.50	426–450	11.75
126–150	6.00	451–475	12.00
151–175	6.75	476–500	12.50
176–200	7.50	501–525	12.75
201–225	7.75	526–550	13.00
226–250	8.00	551–575	13.50
251–275	9.00	576–600	13.75
276–300	9.25	601–up	*
301–325	9.75		

*Add $2.50 for each additional 100 page increment from 601 to 1,000 pages; add $4.50 for each additional 100 page increment over 1,000 pages.

Technical Information Department
LAWRENCE LIVERMORE LABORATORY
University of California | Livermore, California | 94550